Electrochemical Reactions for Electrocoagulation Using Iron Electrodes

Hector A. Moreno C.,[†] David L. Cocke,[‡] Jewel A. G. Gomes,*[,‡] Paul Morkovsky,[§] J. R. Parga,[||] Eric Peterson,[‡] and Cristina Garcia[†]

Instituto Tecnologico de la Laguna, Department of Chemical Engineering, ZC 27000, Torreon, Coahuila, Mexico, Department of Chemical Engineering, Lamar University, P.O. Box 10053, Beaumont, Texas 77710, Kaspar Electroplating Corporation, Shiner, Texas 77984, and Instituto Tecnológico de Saltillo, Department of Metallurgy and Materials Science, V. Carranza 2400, C.P. 25280, Saltillo, Coahuila, México

Electrocoagulation (EC) has been known for more than a century. Applications in industries such as water and wastewater treatment processes have been adapted for the removal of metals, nonmetals, suspended solids, organic compounds, COD (chemical oxygen demand), and BOD (biological oxygen demand). Iron electrodes have been preferred over aluminum due to their durability and cost. However, the electrochemical reactions occurring with EC using iron electrodes have not been systematically studied. For a better understanding of the mechanism and reactions for EC using iron electrodes, we present a review of the concept of green rust (GR) and its relationship to the current theory of EC. Experimental results obtained by measuring pH at different zones near the iron electrodes during the EC process are detailed, and are used to illustrate the mechanism and reactions that occur at both the anode and the cathode. The mechanism and reactions presented explain phenomena associated with EC and are congruent with solubility and Pourbaix diagrams.

Introduction

Electrocoagulation. Electrocoagulation (EC) is an electrochemical technology for the treatment of water and wastewater. In its simplest form, EC uses an electrochemical cell with a dc voltage applied usually to iron or aluminum electrodes, with water or wastewater as the electrolyte.

EC involves the generation of coagulant in situ by dissolution of metal from the anode with simultaneous formation of hydroxyl ions and hydrogen gas at the cathode. This process produces the corresponding aluminum or iron hydroxides and/or polyhydroxides, with the added benefit of the gas generated assisting in bringing the flocculated particles to the surface while providing them additional buoyancy to float at the water surface.

EC was proposed in the 19th century, with a plant successfully erected in London in 1889 for the treatment of sewage. Here wastewater was mixed with seawater and electrolyzed. The EC process was first patented by A. E. Dietrich in 1906 and used to treat bilge water from ships. Three years later, J. T. Harries received a U.S. patent for wastewater treatment by electrolysis using sacrificial aluminum and iron anodes.[1] In the decade of the 1940s, a device known as the "electronic coagulator" electrochemically dissolved aluminum (from the anode) into solution, reacting this with the hydroxyl ion (from the cathode) to form aluminum hydroxide.[2] To purify water, the hydroxide flocculates and coagulates the suspended solids. A similar process was used in Britain in 1956 in which iron electrodes were used to treat river water.[3,4]

While EC was utilized to treat wastewater for most of the 20th century, its success and popularity was exceedingly limited. It was in the final decade where renewed interest was justified. This is evidenced by an increase in the number of EC units sold due to engineering optimizations. The primary advances were in minimizing electrical power consumption and maximizing effluent throughput rates. EC has also been demonstrated to be competitive and effective in the treatment of water and wastewater to remove metals such as Pb, Cd, Cr, As, Mn, Cu, Zn, Ni, Al, Fe, Co, Sn, Mg, Se, Mo, Ca, and Pt. It has also been employed in removing anions such as CN^-, PO_4^{3-}, SO_4^{2-}, NO_3^-, F^-, and Cl^-, nonmetals such as P, organic compounds such as total petroleum hydrocarbons (TPH), toluene, benzene and xylenes (TBX), methyl *tert*-butyl ether (MTBE), chemical oxygen demand (COD), biological oxygen demand (BOD), suspended solids, clay minerals, organic dyes, oil, and greases from a variety of industrial effluents.[1,2,5−9]

Comments about the EC Mechanisms. EC can be considered as an accelerated corrosion process. Its mechanisms are yet to be clearly understood, as there has been little consideration of the factors that influence the effective removal of ionic species and compounds from wastewaters. EC is a complex process with a multitude of mechanisms operating synergistically to remove pollutants from water. A wide variety of opinions exists in the literature for key mechanisms and reactor configurations. A systematic holistic approach is required to understand EC and its controlling parameters.[10]

Most studies have focused on the removal efficiency of a specific pollutant, manipulating parameters such as conductivity, pH, current density, and electrode materials, without exploring the fundamental mechanisms involved in the EC process,[11] particularly those that could provide design parameters to optimize the performance of this relatively simple and inexpensive technique.[12]

Even though EC technology has been used for a considerable period of time, the available literature does not reveal any systematic approach to EC reactor design and operation. This may be due to a lack of sufficient quantitative understanding of the many interactions that occur within an EC reactor and the ability to predict the relative importance of these interactions for a given situation. Studies made for pollutant removal very often prove the viability of the technology but singularly fail to capitalize on its potential by being incorporated within a broad-based understanding of EC technology.[13]

* To whom correspondence should be addressed. Telephone: +409-880-7974. Fax: +409-880-8374. E-mail: jagomes@my.lamar.edu.
[†] Instituto Tecnologico de la Laguna.
[‡] Lamar University.
[§] Kaspar Electroplating Corporation.
[||] Instituto Tecnológico de Saltillo.

10.1021/ie8013007 CCC: $40.75
Published on Web 01/14/2009

EC Challenges. EC has been used for treatment of water and wastewater at both the laboratory and industrial levels. While success has been met within the controlled confines of the laboratory setting, scaling up to meet the requirements of industrial and municipal conditions has proved problematic. The root cause of this situation seems to be that EC is a technology that lies at the intersection of three more fundamental technologies—electrochemistry, coagulation, and flotation. Each of these fields has been studied and possesses a great deal of individual understanding. However, published literature lacks a quantitative appreciation of the way in which these technologies interact to provide optimal EC systems that will foster it into an accepted role as a dependable water treatment technology. Research is required that focuses on explaining, modeling, and quantifying the key interactions and relationships between electrochemistry, coagulation, and flotation.[13]

Green Rust and Current Theory of EC

Rust. Rust is a reddish-brown corrosion product of iron ideally consisting of three layers of iron oxide in different states of oxidation:

Hydrous Ferrous Oxide $FeO \cdot nH_2O$ (or Ferrous Hydroxide $Fe(OH)_2$). The primary corrosion product of iron is $Fe(OH)_2$ (or more likely $FeO \cdot nH_2O$), but the action of oxygen and water can yield other products having different colors.

$$2Fe + O_2 + H_2O \rightarrow 2Fe(OH)_2 \quad (1)$$

$$Fe(OH)_2 + (n-1)H_2O \rightarrow FeO \cdot nH_2O \quad (2)$$

$Fe(OH)_2$, whose color is normally green, turns to greenish-black because of incipient oxidation by air.

Hydrous Ferric Oxide or Ferric Hydroxide. At the outer surface of the corrosion layer, access to dissolved oxygen converts ferrous oxide to hydrous ferric oxide or ferric hydroxide according to the following reaction:

$$4Fe(OH)_2 + O_2 \rightarrow 2Fe_2O_3 \cdot H_2O + 2H_2O \quad (3)$$

This oxide is orange to red-brown in color and comprises most of ordinary rust. It exists as nonmagnetic α-Fe_2O_3 (hematite) or magnetic γ-Fe_2O_3 (maghemite). The α-form possesses a greater negative free energy of formation.[14]

Magnetic Hydrous Ferrous Ferrite. A magnetic hydrous ferrous ferrite, $Fe_3O_4 \cdot nH_2O$, often forms as a black intermediate layer between hydrous Fe_2O_3 and FeO.

$$Fe_2O_3 + FeO \rightarrow Fe_3O_4 \quad (4)$$

Green Rust (GR). GRs are layered Fe(II)−Fe(III) hydroxides having a pyroaurite-type structure consisting of alternating positively charged hydroxide layers and hydrated anion layers. Some of the Fe(II) of the octahedral sheets of $Fe(OH)_2$ is replaced by Fe(III). This results in positive layers of charge that are balanced by the inclusion of anions between the layers.[15] Its exact nature depends on the interlayer anion. Various forms have been synthesized and studied. Results of many studies have shown that GR conforms to a general chemical composition and stoichiometry, that can be represented with the general formula $[Fe^{II}_{(6-x)}Fe^{III}_x(OH)_{12}]^{x+}[(A)_{x/n} \cdot yH_2O]^{x-}$, where x ranges from 0.9 to 4.2, A is an n-valent anion (typically CO_3^{2-}, Cl^-, or SO_4^{2-}), and y denotes the varying amounts of interlayer water (typically y ranges from 2 to 4 for most GRs.[16]

The literature distinguishes between GR-I ($A^{n-} = F^-$, Cl^-, Br^-, I^-), GR-II ($A^{n-} = SO_4^{2-}$), and GR-CO_3 ($A^{n-} = CO_3^{2-}$). This division is due to a crystallographic classification of the mineral structures by which GR-I is described as rhombic, obtained with "planar" anions such as chlorides, carbonate, etc. GR-II and GR-CO_3 are hexagonal; obtained with three-dimensional tetrahedral anions such as sulfate or selenate.[17]

GRs, unlike most iron oxide forms, have an internal surface area; so these minerals have both large specific surface areas and reactivity. Most of the work reported to date has focused on the reactivity of sulfate GR rather than the chloride or carbonate forms.[18] They represent reactive ion exchangers and sorbents.[19] The amphoteric surface hydroxyl groups lead to sorption of both heavy metals (cations) as well as organic anions, e.g. linear alkyl benzene sulfonates (LAS), the major synthetic surfactant used in laundry detergents and cleaning products worldwide, and inorganic anions, e.g. silicate, arsenate, and selenate. Furthermore, polar noncharged compounds are sorbed into the interlayer. Cations such as Cu(II), Ni(II), Zn(II), Cd(II), Co(II), and Mg(II) may isomorphically substitute for Fe(II) during GR formation (coprecipitation). For example, nickelous−ferric GR rusts, the end products obtained by substitution of Fe(II) ions by Ni(II) ions, have been reported.[20−23] This incorporation of cationic inorganic contaminants into the structures of GR could provide an effective means of sequestering contaminants in the subsurface.

GR is now recognized as an important intermediate phase in corrosion of Fe(0). The oxidation of the Fe^{2+} ions in GR results in the formation of ferrihydrite ($Fe_5HO_8 \cdot 4H_2O$), goethite (α-FeOOH), akaganeite (β-FeOOH), and lepidocrocite (γ-FeOOH) in well-aerated systems, and hematite (α-Fe_2O_3), maghemite (γ-Fe_2O_3), or magnetite (Fe_3O_4) in oxygen-depleted systems. Conversion depends on pH, solution composition, oxidant, rate of oxidation, and the degree and rate of dehydration.[24,25] Rust composition, therefore, changes with time (and metal composition). On pure iron, γ-FeOOH transforms to the more stable goethite (α-FeOOH) and some spinel. With increasing time, goethite converts to either maghemite or hematite. Conversion to hematite usually requires higher temperatures.

GRs are formed by a number of abiotic and biotic processes under circumneutral to alkaline conditions in suboxic environments. GRs are believed to play a central role in the redox cycling of Fe in aquatic and terrestrial environments.

Various processes have been developed to synthesize GR in the laboratory. Two primary procedures were envisioned, one by partial oxidation of Fe(II) hydroxides or Fe(II) solutions, and the other by mixing Fe(II) and Fe(III) aqueous solutions or suspensions (coprecipitation). The anion associated with Fe(II) or Fe(III) in the salt is thus present in solution and induces the formation of the corresponding GR; for example, using $FeSO_4$ leads to GR-SO_4. Géhin and co-workers[26] reported that the composition of GR-SO_4 prepared by coprecipitation is the same as that observed for GR-SO_4 samples prepared by other methods. Legrand et al.[17] described new carbonate green rust obtained electrochemically. GR can also be produced with EC. The composition of pollutants in water or wastewater affects both the generation and the type of GR formed.[9]

From sections 1.1 and 1.3, it can be recognized that there are many similarities in reactions that can be achieved and in pollutants that can be removed with GR and EC. One of the factors often used to visually determine the success of pollutant(s) removal with EC using Fe electrodes is the formation of a dark green floc (Figure 1).

Current Theory of EC. The current theory of EC states that it involves several successive stages:[3,12]

(1) Generation of Metal Ions. An iron electrode forms either Fe(II) or Fe(III) at the anode, as shown below:

Anode:

$$Fe \leftrightarrow Fe^{2+} + 2e^- \quad (5)$$

$$Fe \leftrightarrow Fe^{3+} + 3e^- \quad (6)$$

(2) Hydrolysis of Metal Ions and Generation of Metal Hydroxides and Polyhydroxides. This has been studied and explained repeatedly for coagulation processes in water treatment. In the following, the hydrolysis of iron is depicted:

$$Fe + 6H_2O \rightarrow Fe(H_2O)_4(OH)_2(aq) + 2H^+ + 2e^- \quad (7)$$

$$Fe + 6H_2O \rightarrow Fe(H_2O)_3(OH)_3(aq) + 3H^+ + 3e^- \quad (8)$$

(3) Electrolysis of Water. Water is also electrolyzed in a parallel reaction, producing small bubbles of oxygen at the anode and hydrogen at the cathode, and as a result, flotation of the coagulated particles occurs.

Anode:

$$2H_2O(l) \rightarrow O_2(g) + 4H^+ + 4e^- \quad (9)$$

Cathode:

$$2H^+ + 2e^- \rightarrow H_2(g)\uparrow \quad (10)$$

Although the presence of magnetite and maghemite identified in EC sludge when iron electrodes are used might suggest the evolution of oxygen at the anode, this is not the fact during EC with iron electrodes. The experimental evidence for no formation of oxygen during EC with iron electrodes was reported elsewhere.[27] The iron oxides are formed through dehydration of iron hydroxides, and the rust formation partially occurs on the surface of the floated sludge. It can also occur during the separation and analysis processes of the floc, such as filtration and sample preparation.

(4) Destabilization and Aggregation. Destabilization of the contaminants, particulate suspension, breaking of emulsions, and aggregation of the destabilized phases to form flocs through compression of the diffuse double layer and charge neutralization of the ionic species present occurs. Therefore, suspended solids and colloids in small quantities are easily removed by EC.

(5) Physicochemical Reactions. The following physicochemical reactions may also take place in the EC cell: chemical reaction and precipitation of metal hydroxides with pollutants, cathodic reduction of impurities or metal ions present, electrophoretic migration of ions, oxidation of pollutants to less toxic species, and other electrochemical and chemical processes.

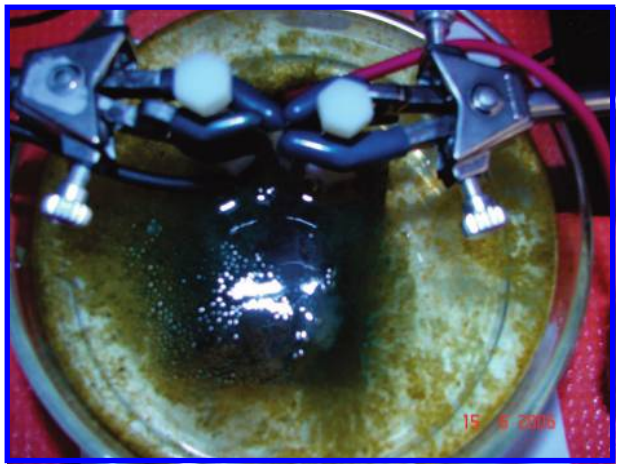

Figure 1. Green rust generated with EC using Fe electrodes.

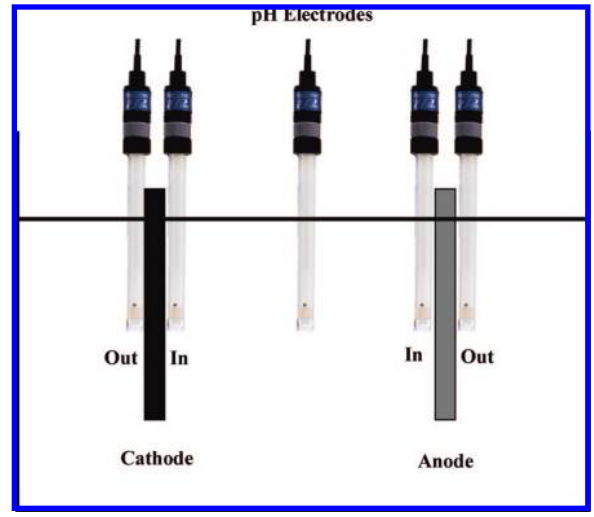

Figure 2. Diagram of the setup used for the first set of experiments showing the position of the pH electrodes in the EC reactor.

Figure 3. Diagram of the setup of pH electrodes on the iron plate (anode and cathode).

Experiments

Three sets of experiments were performed to determine the electrochemical reactions for EC using a 125 × 65 mm^2 Pyrex crystallizer as the cell, 30 × 60 × 2 mm^3 iron plates as electrodes, pH meters (Oakton pH 10 series, Fisher digital 107, Fisher Accumet 125, Barnant Co. model 500-2324, and a Cole Parmer model 607), a UL-CSA direct plug-in transformer unit (with 120 V, 60 Hz, and 6 W input and 12 DCV and 300 mA output), and two multimeters (Cen-tech p-30756 and a CSI/SPECO DMR-2012A). Each set of experiments was performed three times. The pH data shown in Figures 6, 8, and 10 indicate the average of these three values. In general, the standard deviation (1σ) was found to be within 2% of the average values. 0.02 N sulfuric acid and 0.5 g/L of NaCl were used as electrolytes. Reagent grade chemicals and buffers were used.

Experiment 1. Experiment 1 was performed using the setup as shown in Figure 2. Two pH electrodes were placed in the vicinity of the anode, two were in the vicinity of the cathode,

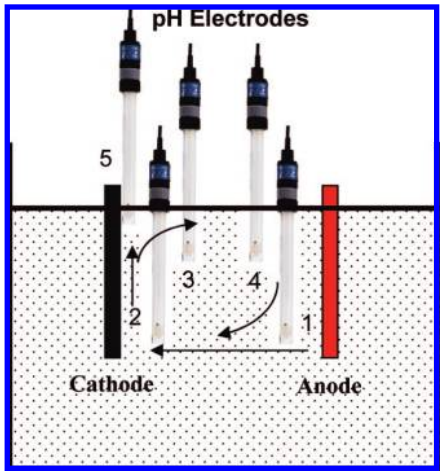

Figure 4. Migration and electrophoretic motion in the EC reactor and location of the pH electrodes.

Figure 5. Generation of sludge around the cathode of the EC reactor.

and the fifth one was in between them. This experiment was carried out without stirring and with three replicates. All three replicates were made under the same voltage and current (12 V and 300 mA).

Experiment 2. Based upon conclusions derived from the first set of experiments, some modifications were made in the setup to track the pH at different locations of the surface of both anode and cathode to explore the electrochemical reactions that take place in the EC reactor and that also correspond to the thermodynamically predominant form of iron under a given set of potential and pH values, i.e., the iron Pourbaix diagram. A schematic of the pH electrode setup is presented in Figure 3. Five pH electrodes were used for the anode, and six pH electrodes were used for the cathode. The sixth pH electrode was required for the cathode to study the pH change at the location where green rust is formed. The positions of the pH electrodes in the vicinity of the EC electrodes were as follows: two pH electrodes (1 and 2) were located on the outside of both anode and cathode, three pH electrodes (3, 4, and 5) were located at different vertical distances near the inner vicinity of the anode, and in a similar fashion four (3, 4, 5, and 6) were placed at different vertical distances near the inner vicinity of the cathode. The inner vicinity indicates the region between the anode and the cathode.

Experiment 3. Since there was no stirring during experiments 1 and 2, it was possible to observe a migration and electrophoretic current in the reactor, as shown in Figure 4. A third experiment was completed to measure the pH along the current path. The pH electrodes were placed at different locations between the anode and the cathode, as shown in Figure 4.

Results and Discussion

It is found from experiment 1 that, for the cathode, the pH vs residence time curves were different, implying that pH varies with the position of the pH electrode over the iron plate and with the oscillatory behavior of the pH observed. For the anode, the time varying pH curves approximate a similar trend, without the oscillatory behavior. At the portion of the anode external to the electric field of the cell, the pH increases slowly up to a value of 4, corresponding to the neutralization of strong acids. Subsequently, the rate of the pH increase accelerates. Finally, sludge generation occurs at the surface of the electrolyte around the cathode, as shown in Figure 5.

Results from experiment 2 are shown in Figures 6−8. Figure 6 shows a plot of pH vs residence time at different locations on the anode. Two ranges or areas of pH are well defined: one that goes from negative pH to pH = 0, and the other that begins at pH 4 and slowly increases to pH 10. It is also known that there is no oxygen evolution at the anode.

These two areas have been highlighted in the iron Pourbaix diagram (Figure 7). The region of negative pH, which is parallel and below the oxygen evolution line, indicates that only Fe(III) ions are being released from the anode. In contrast, the corresponding region from pH = 4 to pH = 10 indicates that Fe(III) hydroxide is also being formed.

The pH vs residence time at different locations on the cathode is plotted in Figure 8. In Figure 8, two different ranges or areas are defined: one that goes from negative pH to pH = 2, and the other that begins at pH 2 and oscillates from low acid to high alkaline values, showing an increasing trend. The plot may not accurately represent the actual behavior because readings were taken within ten minute intervals, and only the uppermost and lowest values were recorded. Another issue is the different sensitivity of the pH meters used.

Knowing that there is hydrogen evolution at the cathode, these areas were highlighted in the iron Pourbaix diagram as shown in Figure 9. The region corresponding to negative pH to pH = 2, parallel and in contact with the hydrogen evolution line, indicates that only Fe(II) ions are being released from the cathode in that part of the electrode. The region corresponding from pH = 2 to pH > 14 indicates that both Fe(II) ions and Fe(II) hydroxide are being generated.

Results from experiment 3 are presented in Figure 10. The plot in Figure 10 corroborates the observation concerning the migration and electrophoretic current. The curve for electrode 1 indicates that there is a high concentration of acidic ions (Fe(III) and $[H^+]$) near the anode. Data for electrodes 2 and 3, both closer to the cathode, indicate a high concentration of acidic ions but less than that for electrode 1. This suggests that some of them are being neutralized in that region. The plot for electrode location 4 shows a pH value of 4 and greater, indicating that strong acid $[H^+]$ has been neutralized. Electrode 5 was located on the surface of the electrolyte close to the cathode, precisely where sludge generation takes place. The corresponding curve shows oscillatory behavior from acid to high alkaline, presenting appropriate pH conditions for precipitation of iron hydroxides.

Electrochemical Reactions in the EC Cell. The electrochemical reactions in the EC reactor must match the observations and data described in the preceding section. Although all reactions are simultaneous, it is easier to explain them if they are presented in sequential order.

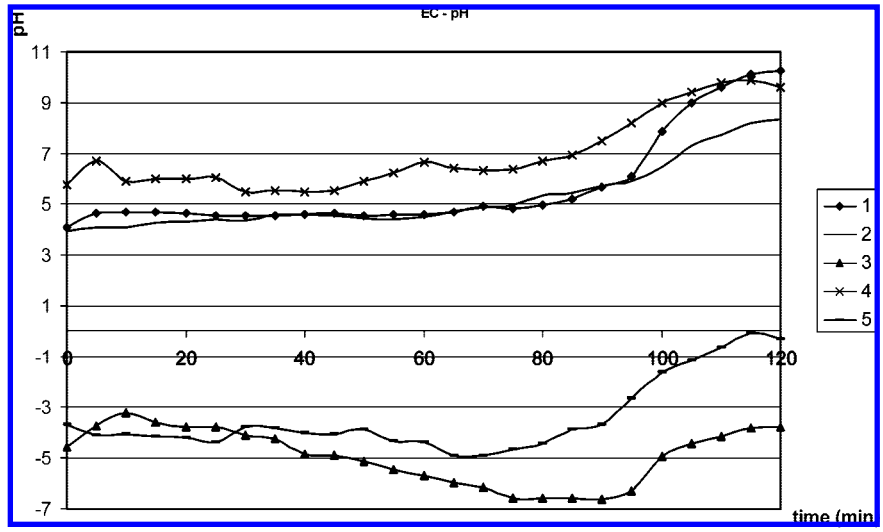

Figure 6. Plot of pH vs residence time at different locations on the anode.

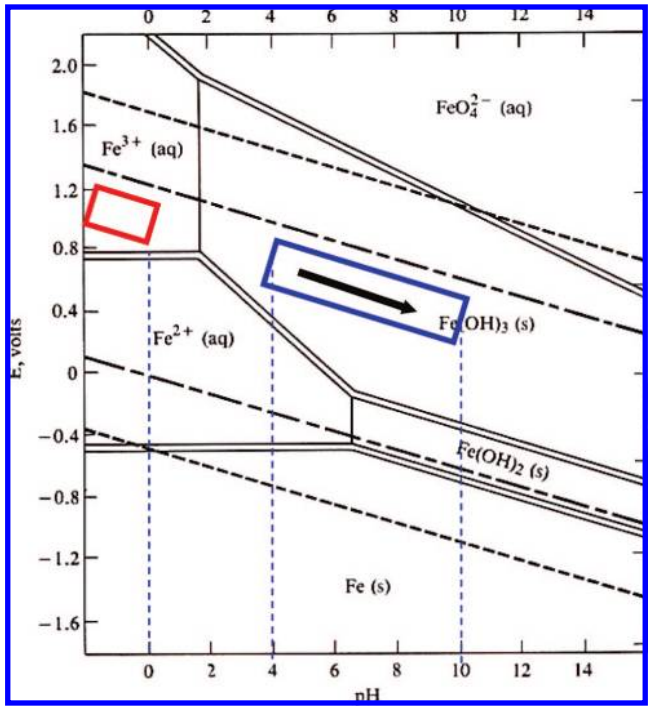

Figure 7. Pourbaix diagram showing the regions in which the anode operates. After M. Pourbaix (1974).[28]

Dissolution of Iron at the Anode. Lorenz et al.[29] experimentally found that the dissolution and passivation rate of iron strongly depends on the electrode potential, the composition of the electrolyte, and the pH. Considering kink sites and monatomic step atoms on the substrate, Lorenz et al.[30] and Keddam[31] proposed the following iron dissolution mechanism:

$$Fe_{kink} + H_2O \rightarrow Fe_{kink}(OH)_{ad} + H^+ + e^- \quad (11)$$

$$Fe_{step} + H_2O \rightarrow Fe_{step}(OH)_{ad} + H^+ + e^- \quad (12)$$

$$Fe_{step}Fe_{kink}(OH)_{ad} \rightarrow Fe_{kink}(OH)_{ad} + Fe^{2+} + 2e^- \quad (13)$$

$$Fe_{kink}Fe_{kink}Fe_{step}(OH)_{ad} \rightarrow Fe_{kink}(OH)_{ad} + Fe_{kink} + Fe^{2+} + 2e^- \quad (14)$$

According to this mechanism, in the rate-determining dissolution charge-transfer step (eq 13), the kink site iron atom, Fe_{kink}, is reproduced by an adjacent iron step atom Fe_{step}. This process corresponds to a movement of kink sites along a monatomic step. Equation 14 indicates the dissolution of a step atom and the generation of two new kink sites.

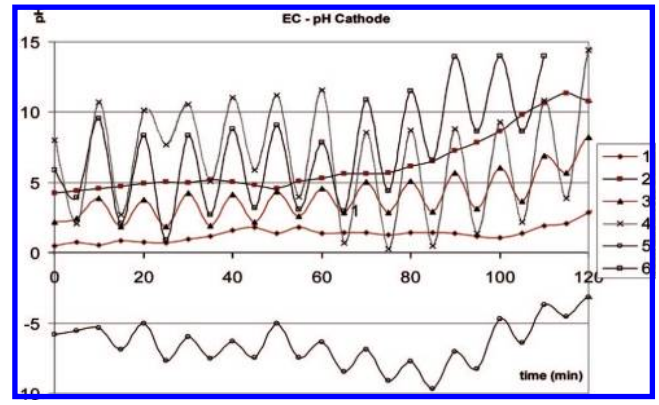

Figure 8. Plot of pH at different locations on the cathode.

If the electrochemical series is considered, the following oxidation potential values are observed for the iron dissolution steps:[32]

$$Fe \leftrightarrow Fe^{2+} + 2e^- \qquad 0.45\ V \quad (5)$$

$$Fe^{2+} \leftrightarrow Fe^{3+} + e^- \qquad -0.77\ V \quad (15)$$

Overall,

$$Fe \leftrightarrow Fe^{3+} + 3e^- \qquad 0.04\ V \quad (6)$$

As shown in the Pourbaix diagram displayed as Figure 8, since the applied potential for EC is greater than 2 V and the pH of the initial aqueous solution is very low (highly acidic), the overall oxidation of Fe to Fe^{3+} is thermodynamically favored. Fe^{3+} ions generated at the anode are strongly attracted to the stationary cathode and move toward it.

Bulk Solution (on the Way to the Cathode). If there is a strong acid present, Fe(III) ions will first react with the anions associated with the acid. In this particular case:

$$2Fe^{3+} + 3SO_4^{2-} \rightarrow Fe_2(SO_4)_3(aq) \quad (16)$$

After neutralization of strong acids via hydrogen evolution, hydrolysis of Fe(III) will occur:

$$Fe^{3+} + H_2O \rightarrow Fe(OH)^{2+} + H^+ \quad (17)$$

$$Fe(OH)^{2+} + H_2O \rightarrow Fe(OH)_2{}^+ + H^+ \quad (18)$$

$$Fe(OH)_2{}^+ + H_2O \rightarrow Fe(OH)_3 + H^+ \quad (19)$$

According to the density-functional theory study performed by Abreu et al.,[33] the hydrated form of $Fe(OH)_2{}^+$ was found to be the most stable species among Fe(III) hydrolysis products. Therefore, we assume that it is primarily this species which migrates to the cathode in addition to the generated H^+ ions.

Cathode. Hydrogen is evolved at the cathode:

$$2H^+ + 2e^- \rightarrow H_2(g)\uparrow \quad (10a)$$

The rate of reaction depends on the removal of $[H^+]$ via H_2 evolution. This reaction will occur fast for low pH values (strong acids).[34]

If a strong acid is present (sulfuric acid in this case), it will provide the hydrogen ions for the hydrogen evolution reaction until it is completely reacted. After neutralization of strong acids, the hydrogen ions are provided by hydrolysis of iron and possibly by weak acids if present. Oscillatory behavior is produced by hydrogen evolution in concert with the formation of iron(II) hydroxide (high pH) and new H^+ ions attracted to the cathode (low pH).

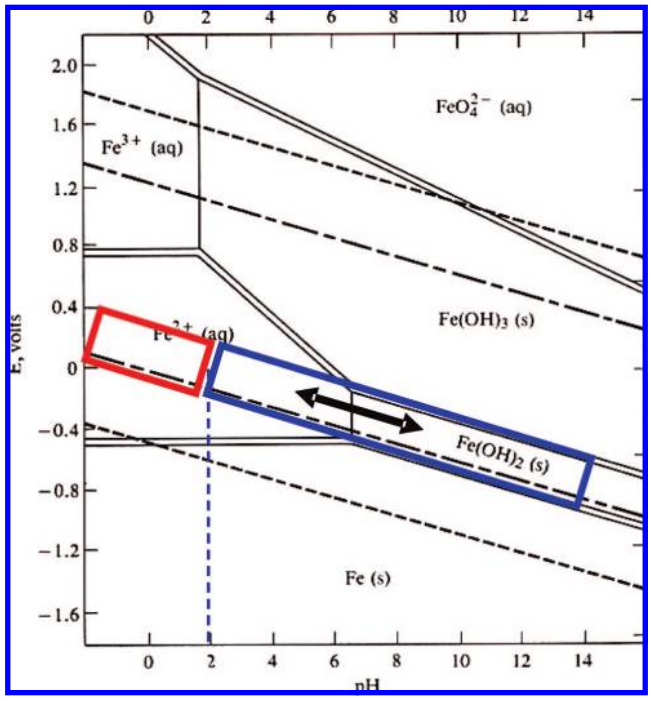

Figure 9. Pourbaix diagram showing the regions in which the cathode operates. After M. Pourbaix (1974).[28]

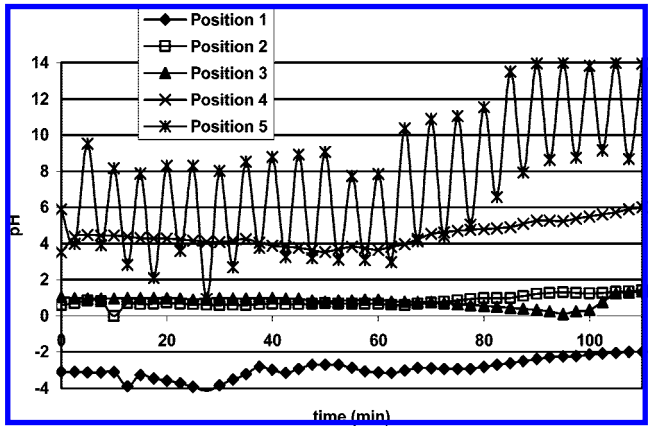

Figure 10. Plot of pH vs residence time for experiment 3.

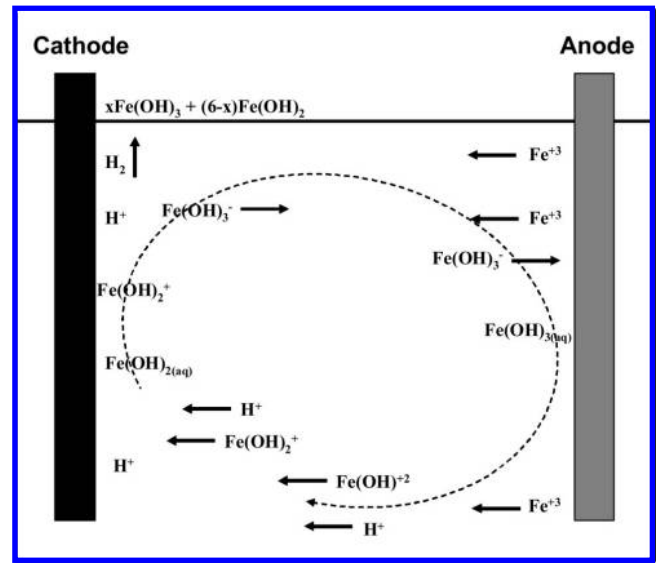

Figure 11. Migration of cations and anions in the EC reactor.

At the cathode, in addition to hydrogen evolution according to experiment 2 and the Pourbaix diagram in Figure 9, generation of Fe(II) and Fe(II) hydroxide occurs as explained by the following reactions.

$$Fe(OH)_2{}^+ + e^- \rightarrow Fe(OH)_2(aq) \quad (20)$$

If the pH is high enough, it may precipitate:

$$Fe(OH)_2(aq) \rightarrow Fe(OH)_2(s) \quad (21)$$

But the hydrolysis could go further:

$$Fe(OH)_2(aq) + H_2O \rightarrow Fe(OH)_3{}^- + H^+ \quad (22)$$

Reaction 22 is favored by the hydrogen evolution reaction (eq 10), and the $Fe(OH)_3{}^-$ ion will be attracted to the anode.

Anode. At the anode, $Fe(OH)_3{}^-$ ion will be converted to $Fe(OH)_3(aq)$ as depicted in reaction 23:

$$Fe(OH)_3{}^- \rightarrow Fe(OH)_3(aq) + e^- \quad (23)$$

Experiment 2 and the Pourbaix diagram in Figure 7 show that there is generation of Fe(III) hydroxide at the anode. Reactions 18 and 19 describe this generation.

Cathode. As previously described, a migration and electrophoretic current is established that vacillates between the anode and cathode. This current also carries $Fe(OH)_3(aq)$ and $Fe(OH)_2(aq)$. Upon finding proper pH conditions at the top of the cathode (Figure 5), these species turn into insoluble iron oxides/hydroxides or oxyhydroxides. Under the appropriate conditions, they combine in the following proportion to generate GR.

Green Rust Formation. In the following, a complete sketch of formation of green rust is reiterated.

$$Fe \leftrightarrow Fe^{3+} + 3e^- \quad \text{(anode)} \quad (6b)$$

$$Fe(OH)^{2+} + H_2O \rightarrow Fe(OH)_2{}^+ + H^+ \quad \text{(bulk solution)} \quad (18)$$

$$2H^+ + 2e^- \rightarrow H_2(g)\uparrow \quad \text{(cathode)} \quad (10)$$

$$Fe(OH)_2{}^+ + e^- \rightarrow Fe(OH)_2(aq) \quad \text{(cathode)} \quad (20)$$

$$Fe(OH)_2(aq) + H_2O \rightarrow Fe(OH)_3^- + H^+ \quad \text{(cathode)} \quad (22)$$

$$Fe(OH)_3^- \rightarrow Fe(OH)_3(aq) + e^- \quad \text{(anode)} \quad (23)$$

Overall Reaction. In general, hydrogen gas and green rust are formed at the cathode as shown in eq 24:

$$6Fe + (12 + x)H_2O \rightarrow {}^1/_2(12 - x)H_2(g)\uparrow + x Fe(OH)_3 \cdot (6 - x)Fe(OH)_2(s) \quad (24)$$

If pH conditions are too acidic or alkaline for the bulk solution, EC will not lead to GR formation and the removal efficiency of pollutants will be small, especially for amphoteric metals. The migration of cations and anions in the EC reactor is schematically shown in Figure 11. It also shows the formation of green rust from the produced ions in EC using Fe electrodes.

Formation of rust (dehydrated hydroxides) also occurs as shown in the following:

$$2Fe(OH)_3 \leftrightarrow Fe_2O_3 + 3H_2O \quad \text{(hematite, maghemite)} \quad (25)$$

$$Fe(OH)_2 \leftrightarrow FeO + H_2O \quad (26)$$

$$2Fe(OH)_3 + Fe(OH)_2 \leftrightarrow Fe_3O_4 + 4H_2O \quad \text{(magnetite)} \quad (27)$$

$$Fe(OH)_3 \leftrightarrow FeO(OH) + H_2O \quad \text{(goethite, lepidocrocite)} \quad (28)$$

Hematite, maghemite, rust, magnetite, lepidocrocite, and goethite have been identified as EC byproducts by Parga et al.[11,35] and Gomes et al.[36] These authors performed EC experiments in stirred or turbulent conditions. Considering the fact of formation of the same EC byproduct for both stirring and nonstirring conditions, it can be stated that the proposed electrochemical reactions obtained by the nonstirred EC reactor can also be applicable for the system with stirred or continuous reactors.

This paper is a result of our continuous research on EC. That is why we did not include here our previous works on measurements of iron species and various results of electrocoagulation.[11,35−37] Our objective was to emphasize the variability of pH during EC at different locations inside the reactor and thereupon to propose reaction schemes for EC with iron electrodes that are compatible with previous thermodynamic and kinetic studies.

Conclusions

The following conclusions can be drawn from the experimental data obtained:

- Oxygen evolution does not take place during EC when using iron electrodes.
- EC is an accelerated corrosion process that may be explained with the iron Pourbaix diagram.
- Observations and data from experiments measuring pH at different locations of both cathode and anode, while running EC without stirring, together with the iron Pourbaix diagram explain the proposed electrochemical reactions occurring in an EC reactor.
- EC is a cyclic dynamic process: pH, concentrations, and species are different in almost every zone of the EC reactor.
- The formation of final EC byproducts involves an intermediate step that generates GR.
- The same electrochemical reactions occur in stirred and continuous reactors.

Acknowledgment

We are greatly thankful for financial support from USDA (2004-38899-02181), Texas ATP (Grant No. 003581-0033-2003), and the Welch foundation (Grant No. V-1103).

Literature Cited

(1) Vik, E. A.; Carlson, D. A.; Eikun, A. S.; Gjessing, E. T. Electrocoagulation of Potable Water. *Water Res.* **1984**, *18* (11), 1355.

(2) Matteson, M. J.; Dobson, R. L.; Glenn, R. W.; Kukunoor, N. S.; Waits, W. H.; Clayfield, E. J. Electrocoagulation and Separation of Aqueous Suspensions of Ultrafine Particles. *Colloids Surf., A* **1995**, *104* (1), 101.

(3) Holt, P.; Barton, G.; Mitchell, C. Electrocoagulation as a Wastewater Treatment. *The 3rd Annual Australian Environmental Engineering Research*, Castlemaine, Victoria, 1999, 23−26 November.

(4) Kaselco, website: http://www.kaselco.com.

(5) Chen, G. H. Electrochemical Technologies in Wastewater Treatment. *Sep. Purif. Technol.* **2004**, *38* (1), 11.

(6) Murugananthan, M.; Raju, G. B.; Prabhakar, S. Separation of Pollutants from Tannery Effluents by Electroflotation. *Sep. Purif. Technol.* **2004**, *40* (1), 69.

(7) Inan, H.; Dimogio, A.; Simsek, H. Olive Oil Mill Wastewater Treatment by Means of Electro-coagulation. *Sep. Purif. Technol.* **2004**, *36* (1), 23.

(8) Chen, M. X.; Chen, G. H.; Yue, P. L. Separation of Pollutant from Restaurant Wastewaters by Electrocoagulation. *Sep. Purif. Technol.* **2000**, *19* (1−2), 65.

(9) Moreno, C. H. A.; Cocke, D. L.; Gomes, J. A. G.; Morkovsky, P.; Parga, J. R.; Peterson, E.; Garcia, C. Electrochemical Generation of Green Rust with Electrocoagulation. *ECS Trans.* **2007**, *3* (18), 67.

(10) Mollah, M. Y. A.; Schennach, R.; Parga, J. R.; Cocke, D. L. Electrocoagulation—Science and Applications. *J. Hazard. Mater.* **2001**, *84* (1), 29.

(11) Parga, J. R.; Cocke, D. L.; Valenzuela, J. L.; Kesmez, M.; Gomes, J. A. G.; Valverde, V. As Removal by EC Technology in the Comarca Lagunera Mexico. *J. Hazard. Mater.* **2005**, *124* (1−3), 247.

(12) Mollah, M. Y. A.; Morkovsky, P.; Gomes, J. A. G.; Kesmez, M.; Parga, J.; Cocke, D. L. Fundamentals, Present and Future Perspectives of Electrocoagulation. *J. Hazard. Mater.* **2004**, *114* (1−3), 199.

(13) Holt, P.; Barton, G.; Mitchell, C. The Future of EC as a Localized Water Treatment Technology. *Chemosphere* **2005**, *9* (I3), 335.

(14) Balasubramanian, R.; Kumar, A. V. R.; Dillman, P. Characterization of Rust on Ancient Indian Iron. *Curr. Sci.* **2003**, *85* (11), 1546.

(15) Bernal, J. D.; Dasgupta, D. R.; Mackay, A. L. The Oxides and Hydroxides of Iron and Their Structural Inter-Relationships. *Clay Miner. Bull.* **1959**, *4* (21), 15.

(16) Chavez, L. H. G. The Role of Green Rust in the Environment: a Review Revista Brasileira de Engenharia. *Agricolae Ambiental* **2005**, *9* (2), 284.

(17) Legrand, L.; Sagon, G.; Lecomte, S.; Chausse, A.; Messina, R. A Raman and Infrared Study of a New Carbonate Green Rust Obtained by Electrochemical Way. *Corros. Sci.* **2001**, *43* (9), 1739.

(18) Williams, A. G. B.; Scherer, M. M. Kinetics of Cr(VI) Reduction by Carbonate Green Rust. *Environ. Sci. Technol.* **2001**, *35* (17), 3488.

(19) Hansen, H. C. B.; Koch, C. B.; Krogh, H. N.; Borggaard, O. K.; Sorensen, J. Abiotic Nitrate Reduction to Ammonium: Key Role of Green Rust. *Environ. Sci. Technol.* **1996**, *30* (6), 2053.

(20) Refait, P.; Génin, J. M. R. The Oxidation of Ni(II)-Fe(II) Hydroxides in Chloride-Containing Aqueous Media. *Corros. Sci.* **1993**, *4* (12), 2059.

(21) Refait, P.; Génin, J. M. R. Mechanisms of Oxidation of Ni(II)-Fe(II) Hydroxides in Chloride-Containing Aqueous Media: Role of the Pyroaurite-Type Ni-Fe Hydroxychlorides. *Clay Miner.* **1997**, *32* (4), 597.

(22) Refait, P.; Drissi, H.; Génin, J. M. R. The Substitution of Fe^{2+} Ions by Ni^{2+} Ions in Green Rust One Compounds. *Hyperfine Interact.* **1994**, *90* (1−4), 389.

(23) Refait, P.; Abdelmoula, M.; Génin, M. R. Oxidation of Pyroaurite-Like Ni-Fe Hydroxychlorides Studied by Mössbauer Spectroscopy at 16 K. *Clay Miner.* **1998**, *33* (4), 665.

(24) Loyaux-Lawniczak, S.; Refait, P.; Ehrhardt, J.-J.; Lecomte, P.; Génin, J.-M. Trapping of Cr by Formation of Ferrihydrite During the Reduction of Chromate Ions by Fe(II)-Fe(III) Hydroxysalt Green Rust. *Environ. Sci. Technol.* **2000**, *34* (3), 438.

(25) Lin, R.; Spicer, R. L.; Tungate, F. L.; Davis, B. H. A Study of the Oxidation of Ferrous Hydroxide in Slightly Basic Solution to Produce γ-FeOOH. *Colloids Surf., A* **1996**, *113* (1−2), 79.

(26) Géhin, A.; Ruby, C.; Addelmoula, M.; Benali, O.; Ghanbaja, J.; Refait, P.; Génin, J. M. R. Synthesis of Fe(II-III) Hydroxysulphate Green Rust by Coprecipitation. *Solid State Sci.* **2002**, *4* (1), 61.

(27) Moreno, H. A.; Cocke, D.; Gomes, J. A.; Morkovsky, P.; Parga, J. Electrocoagulation Mechanism for Metal Removal. *ECS Trans.* **2007**, *2* (13), 51.

(28) Pourbaix, M. *Atlas of Electrochemical Equilibria in Aqueous Solutions*, 2nd ed.; NACE: Houston, 1974.

(29) Lorenz, W. J.; Staikov, G.; Schindler, W.; Wiesbeck, W. The Role of Low-Dimensional Systems in Electrochemical Phase Formation and Dissolution Processes. *J. Electrochem. Soc.* **2002**, *149* (12), K47.

(30) Lorenz, W. J.; Heusler, K. E. Anodic Dissolution of Iron Group Metals In *Corrosion Mechanisms*; Mansfeld, F., Eds. Marcel Dekker: New York, 1987.

(31) Keddam, M. Anodic Dissolution. In *Corrosion Mechanisms in Theory and Practice*; Marcus, P., Ed.; Marcel Dekker: New York, 2002.

(32) Lide, D. R., Editor-in-Chief *CRC Handbook of Chemistry and Physics*, 79th ed.; CRC Press: Boca Raton, 1998.

(33) Abreu, H. A. D.; Guimaraes, L.; Duarte, H. A. Density-Functional Theory Study of Iron(III) Hydrolysis in Aqueous Solution. *J. Phys. Chem. A* **2006**, *110*, 7713.

(34) Corrosion-Doctors, website: http://www.corrosion-doctors.org/Forms-crevice/iron-corrosionX.htm.

(35) Parga, J. R.; Cocke, D. L.; Valverde, V.; Gomes, J. A. G.; Kesmez, M.; Moreno, H.; Weir, M.; Mencer, D. Characterization of Electrocoagulation for Removal of Cr and As. *Chem. Eng. Technol.* **2005**, *28* (5), 605.

(36) Gomes, J. A. G.; Daida, P.; Kesmez, M.; Weir, M.; Moreno, H.; Parga, J. R.; Irwin, G.; McWhinney, H.; Grady, T.; Peterson, E.; Cocke, D. L. Arsenic Removal by Electrocoagulation Using Combined Al-Fe Electrode System and Characterization of Products. *J. Hazard. Mater.* **2007**, *B139*, 220.

(37) Mollah, M. Y. A.; Pathak, S. R.; Patil, P. K.; Vayuvegula, M.; Agrawal, T. S.; Gomes, J. A. G.; Kesmez, M.; Cocke, D. L. Treatment of Orange II Azo-Dye by Electrocoagulation (EC) Technique in a Continuous Flow Cell Using Sacrificial Iron Electrodes. *J. Hazard. Mater.* **2004**, *B109*, 165.

Received for review August 27, 2008
Revised manuscript received November 30, 2008
Accepted December 3, 2008

IE8013007